PERGAMON

International Journal of Multiphase Flow 25 (1999) 1373–1393

International Journal of Multiphase Flow

www.elsevier.com/locate/ijmulflow

Oscillatory transient two-phase flows in single channels with reference to monolithic catalyst supports

N. Reinecke, D. Mewes*

Institut für Verfahrenstechnik, Universität Hannover, Callinstraße 36, D-30167 Hannover, Germany

Received 14 December 1998; received in revised form 1 March 1999

Single and parallel channels are items in which Gad Hetsroni's interests and ours met many years ago. A very good relationship developed between the process engineering research group in Hannover and his group at the Technion. We are very thankful for many ideas he transferred to us and the many critical and very constructive discussions during which we established a very good cooperation during the past years. Best wishes to Gad for the next years, good health and ideas for enthusiastic research in multiphase flow.

Abstract

Investigations of transient two-phase flow oscillations in single channels and monolithic catalyst supports are described. The experimental investigations were conducted in glass capillaries of varying inner diameter as well as ceramic monoliths. As a result of the experimental investigations pressure drop instabilities were found both in reference to the liquid and the gaseous phase. When coupling the test sections with compressible volumes in the feedlines of the phases pressure drop oscillations of the two-phase flow are established. A model is presented for the theoretical description of the resulting transient flow oscillations. The basis for the model are the momentum and mass conservation equations for all the components. For the flow instability developing in the test section experimental results are used. The non-linear differential equations of second order are solved by a dynamic finite step numerical scheme. The experimental and the theoretical results for the pressure drop oscillations are compared.

Keywords: Two-phase flow; Capillary; Monolith; Transient; Oscillation; Pressure drop instability

* Corresponding author. Tel.: +49-511-762-3638; fax: +49-511-762-3031.
E-mail address: dms@c36.uni-hannover.de (D. Mewes)

0301-9322/99/$ - see front matter
PII: S0301-9322(99)00046-4

1. Introduction

Regular and irregular packings are used in the chemical industry for a variety of different mass-transfer and reaction applications. Most of the heterogeneous reactions of multiphase systems are carried out using wetted catalysts. For the conversion rate in such a system, the mass-transfer resistance into and through the liquid phase as well as the kinetics of the reaction at the surface of the solid catalyst are influential. In order to reduce the mass-transfer resistance in the liquid phase, turbulences are desirable. These are easily obtained for countercurrent reactors such as distillation and rectification columns. In the case where an excessive reaction is possible, for instance, in hydrogenation of a variety of components or hydro-treatment, the cocurrent downflow of the gaseous and the liquid phase is chosen.

In Fig. 1, two possible reactors for cocurrent downflow of the two phases are schematically shown. The reactors consist of a tray (1) holding the packing or the monoliths (2) and a feed for both phases at the top of the column as well as a separation unit for the phases at the bottom. For certain flow rates of the phases, a region of bubbles in a continuous liquid will establish above the catalyst. In this region a high turbulent mixing of both phases can be observed.

In the case of trickle-bed reactors as shown in Fig. 1a, a high level of turbulence within the

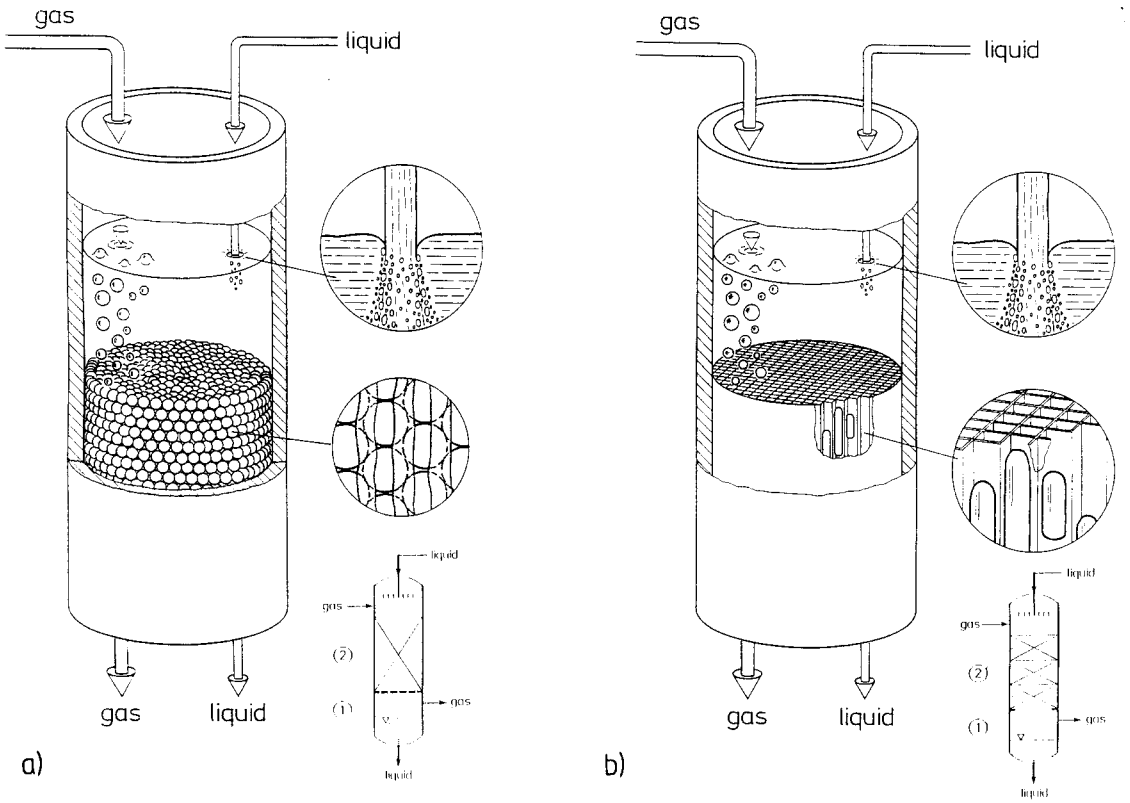

Fig. 1. Schematical representation of (a) a trickle-bed reactor and (b) a monolithic reactor.

liquid phase in the column is generated for the pulse flow regime of the two phases. The pulse flow is obtained due to instabilities of the flow through the packing and subsequent blocking of the passages for the gaseous phase by the liquid. The experimental and theoretical investigations regarding the onset, development and mapping of the pulse flow in trickle-bed reactors are numerous, for example, Gianetto et al., 1978; Gianetto and Specchia, 1992; Holub et al., 1992, 1993; Talmor, 1977; Morsi et al., 1984; Chou et al., 1977; Sai and Varma, 1988; Grosser et al., 1988. Even though the mass transfer in this regime is significantly increased, the pressure drop of the flow through irregular packings is also increased resulting in high operating costs. Recently, an alternative to the irregular packings in trickle-bed reactors has been developed. The application of monolithic catalysts for two-phase cocurrent flow is advantageous because of the regularity of the packing and the resulting low pressure drop. In the case of monolithic reactors though, as shown in Fig. 1b a distinct pulse flow regime is not observed. Yet for higher flow rates of both phases oscillatory flow instabilities develop, leading to pressure drop oscillations of the system. Since the mass-transfer in this flow regime is significantly increased, the knowledge of the physical reasons for the onset of the oscillation and the physical properties of the developing transient flow are important.

2. Two-phase flow in monoliths and single channels

The application of monolithic catalysts for gas phase reactions and two-phase hydrogenation reactions has been reported by a number of authors including Hatziantoniou and Anderson (1982, 1984); Kawakami et al. (1989); Irandoust and Anderson (1988, 1989a, b); Irandoust et al. (1989); Irandoust and Gahne (1990); Tronconi et al. (1991); Tronconi and Forzatti (1992); Svachula et al. (1993a, b); Beretta et al. (1993); Crynes et al. (1995). The experimental investigations were carried out using monoliths and single channels. The flow regime encountered in the multiphase systems was exclusively the bubble flow regime which is established for small flow rates of the phases.

A systematic characterization of the possible flow regimes of cocurrent two-phase flow in the monoliths was carried out by Satterfield and Özel (1977). They showed that the flow in the single vertical channel of the monolith can be characterized by a two-phase flow in vertical capillaries. The encountered flow regimes were annular flow, bubble flow and slug flow. The investigations were not extended to higher flow rates of the two phases. Crynes et al. (1995) studied a monolithic froth reactor with a cocurrent upflow of the two phases but their entrance conditions are a froth layer of the two phases. Suo (1968) and Suo and Griffth (1964), as well as Marchessault and Mason (1960), Kariyasaki et al. (1991), Thulasidas et al. (1995), Irandoust and Anderson (1989a, b) also studied the two-phase flow in capillaries. The predominant flow regime was the bubble or the slug flow regime. It was found, that the void fraction only deviates slightly from the fraction of the volumetric gas flow rate in the total flow rate. For the small superficial velocities of the phase that were studied, no pressure drop instabilities were found. Ozawa et al. (1979a, b, c, 1982, 1984) studied the two-phase flow in horizontal capillary tubes for slightly higher flow rates and found that for the transition between the bubble and the slug flow regime, an instable region of the pressure drop is encountered. The combination of a single or two or more instable test sections with compressible buffer volumes leads to

pressure drop oscillations of the flow rates of both phases. The analytical description of the system with a lumped parameter model leads to qualitatively good results yet errors for the absolute values of the amplitude and the frequency of the oscillations.

3. General description of the oscillations

The behaviour of a test section with a pressure drop instability coupled to a stable feed system containing buffer volumes is schematically shown in Fig. 2. In Fig. 2a the feed system and the instable test section is shown. For simplicity, a single phase system is considered. The feed system consists of a buffer volume and a feed pipe, both with stable behaviour. The only external input into the system is a mass flow rate $\dot{m}_1$ which is kept constant. The mass flow rate $\dot{m}_1$ is supplied at an arbitrary pressure p_1 which can vary independently of the flow rate. It is assumed, that a dynamic coupling between the considered system and the feed pumps can be neglected. At the junction the feed mass flow rate $\dot{m}_1$ is divided into the mass flow rates $\dot{m}_2$ flowing into the buffer volume and $\dot{m}_3$ flowing through the feed pipe. The mass flow rate $\dot{m}_3$ enters the instable test section at point 2. The test section shows a pressure drop instability

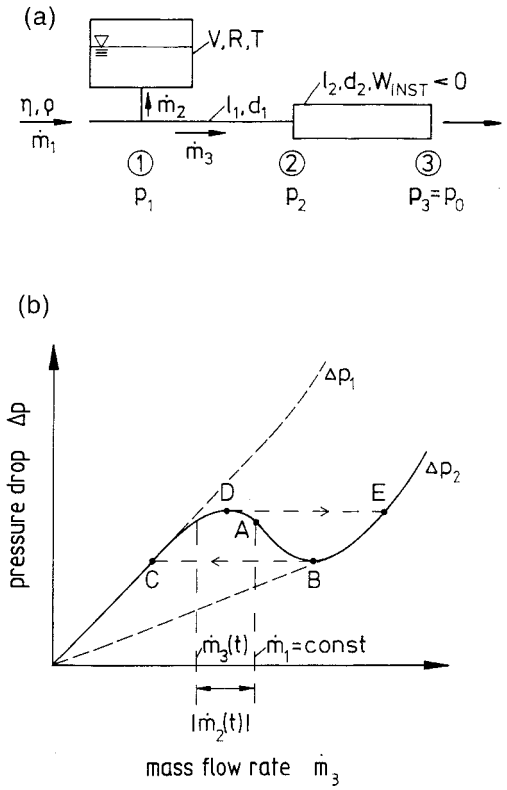

Fig. 2. Schematical representation of a system with pressure drop instabilities: (a) setup and (b) pressure drop instability.

which is schematically shown in Fig. 2b. Plotted is the pressure drop of the test section as a function of the mass flow rate $\dot{m}_3$. It is assumed, that the pressure drop of the test section changes from an asymptote Δp_1 for small mass flow rates to an asymptote Δp_2 for large mass flow rates via instable operating points between D and B where

$$\frac{\mathrm{d}\Delta p}{\mathrm{d}\dot{m}_3} < 0 \tag{1}$$

When a constant mass flow rate $\dot{m}_1$ is supplied by the feed at a given operating point A, a very small increase of the mass flow rate into the test section $\dot{m}_3$ will result in a decreasing pressure drop. As the pressure drop across the test section decreases, the pressure just outside the buffer volume p_1 decreases also, leaving a driving pressure gradient between the buffer volume and the junction. Thus, the mass flow rate $\dot{m}_2$ is discharged from the buffer volume. The additional mass flow rate increases the mass flow rate $\dot{m}_3$ further yielding an even smaller pressure drop across the test section. This dynamic behaviour will continue until the operating point B is reached. At this point the system is again stable but due to the inertia of the system the mass flow rate $\dot{m}_3$ will be increased further in direction of E. When the pressure inside the buffer volume is equal to the pressure at the junction, the dynamic behaviour of the system is reversed. Now, the buffer is depleted of the flowing medium and has to be recharged. The operating point therefore moves back toward point B and then very fast through the instable region to operating point C. This very mast movement of the operating point results in an almost transient change of flow rate. At operating point C, the mass inside the buffer volume is discharged into the test section and the operating point moves toward D. Since at point D a similar behaviour than in point B is encountered an oscillation developes.

In order to estimate the effect of a variation of the parameters, a simple formulation of the problem can be used. The pressure drop of the feed pipe is calculated using a laminar friction law and a mechanistic acceleration formulation of the form

$$p_1 - p_2 = W_1 \dot{m}_3 + W_{2,1} \frac{\mathrm{d}\dot{m}_3}{\mathrm{d}t} \tag{2}$$

where the coefficient W_1 can be calculated by

$$W_1 = \frac{128}{\pi} \frac{l_1}{d_1^4} \frac{\eta}{\rho} \tag{3}$$

with l_1 as the length of the pipe, d_1 the diameter, ρ the density and η the dynamic viscosity of the flowing medium. The coefficient $W_{2,1}$ can be calculated by

$$W_{2,1} = \frac{4}{\pi} \frac{l_1}{d_1^2} \tag{4}$$

The pressure drop of the instable test section will only be considered in the instable operating region. This yields the simple formulation:

$$p_2 - p_3 = \Delta p_0 - |W_{\mathrm{INST}}| \dot{m}_3 + W_{2,2} \frac{\mathrm{d}\dot{m}_3}{\mathrm{d}t} \tag{5}$$

The pressure drop Δp_0 is an initial pressure drop which is reduced by a pressure drop calculated with W_{INST}. The acceleration pressure drop is calculated analogous to the feed pipe by using

$$W_{2,2} = \frac{4}{\pi}\frac{l_2}{d_2^2} \tag{6}$$

where l_2 and d_2 are the length and diameter of the test section, respectively. The behaviour of the compressible buffer volume is described using the ideal gas law

$$\frac{\mathrm{d}p_1}{\mathrm{d}t} = W_3 \dot{m}_3 \tag{7}$$

with the coefficient W_3 containing

$$W_3 = \frac{RT}{V} \tag{8}$$

In Eq. (8), R is the specific gas constant, V the size of the buffer volume and T the absolute temperatures. Eqs. (2)–(8) are coupled using a balance of the mass flows at point 1:

$$\dot{m}_1 = \dot{m}_2 + \dot{m}_3 \tag{9}$$

When Eqs. (2)–(9) are introduced into one another and rearranged, an inhomogeneous differential equation of second order is obtained. In order to estimate the effect of a variation of parameters, the homogeneous solution is considered. The differential equation is thus reduced to

$$A\frac{\mathrm{d}^2\dot{m}_3}{\mathrm{d}t^2} + B\frac{\mathrm{d}\dot{m}_3}{\mathrm{d}t} + C\dot{m}_3 = 0 \tag{10}$$

The coefficients in Eq. (10) can be calculated by

$$A = W_{2,1} + W_{2,2} \tag{11}$$

$$B = W_1 - |W_{\mathrm{INST}}|$$

and

$$C = W_3 \tag{13}$$

From the differential equation given in Eq. (10) it is evident, that the flow in the test section behaves as a linear, damped, harmonic oscillator. It is assumed that the given eigenvalues of the system are stable and no amplitude enhancement takes place. Therefore, the linear solution of the differential equation is

$$\omega_0 = \sqrt{\frac{C}{A}} = \sqrt{\frac{W_3}{W_{2,1} + W_{2,2}}} \tag{14}$$

The linear cycle frequency ω_0 is defined as

$$\omega_0 = 2\pi f = \frac{2\pi}{T} \tag{15}$$

where f is the oscillation frequency and T the period of oscillation. The damping coefficient D is calculated by

$$D = \frac{B}{2\sqrt{cA}} = \frac{W_1 - |W_{\mathrm{INST}}|}{2\sqrt{W_3(W_{2,1} + W_{2,2})}} \tag{16}$$

The actual oscillation cycle frequency ω_δ is then

$$\omega_\delta = \omega_0\sqrt{1 - D^2} \tag{17}$$

Using Eqs. (14), (16) and (17) the effect of a variation of parameters can be estimated.

1. Volume of the buffer V: An increase of the buffer volume V will lead to a decrease of parameter W_3. This will result in a subsequent decrease of the linear cycle frequency ω_0 as well as an increase of the damping coefficient D. The result is a total decrease of the oscillation cycle frequency ω_δ.
2. Friction of the feed pipe: An increase of the friction within the feed pipe will result in an increase of parameter W_1. This will result in an increase of the dumping coefficient D and a resulting decrease of the oscillation cycle frequency ω_δ.
3. Slope of the region of instability: An increase of the slope of the pressure drop curve in the instable region will result in an increase of parameter W_{INST}. This will result in a decrease of the damping coefficient D and an increase of oscillation cycle frequency ω_δ.

As the size of the buffer volume is decreased down to zero, the frequency of the oscillation becomes infinity, while the enhancement of the amplitude of the oscillation approaches 1. Therefore, in the absence of compressibilities in the feed lines, a measurement of stationary pressure drop curves is possible.

4. Experimental investigations

In order to examine the two-phase cocurrent downflow in vertical capillaries experimental investigations were performed. The experimental investigation that were conducted were grouped in two stages. First, the stationary pressure drop characteristic of the two-phase flow in a capillary was investigated. For these investigations it is necessary to have no compressible buffer volumes in the feed lines of the supply system. In a second stage, compressible volumes for either or both phases were introduced into the feed system and the resulting pressure drop oscillations monitored.

In Fig. 3 the experimental setup is schematically shown. The test section consists of a glass or perspex capillary with an inner diameter of 3 and 2 mm (round cross-section) or 1.5 mm (square cross-section). The total length of the test section is 1000 mm. The capillaries are

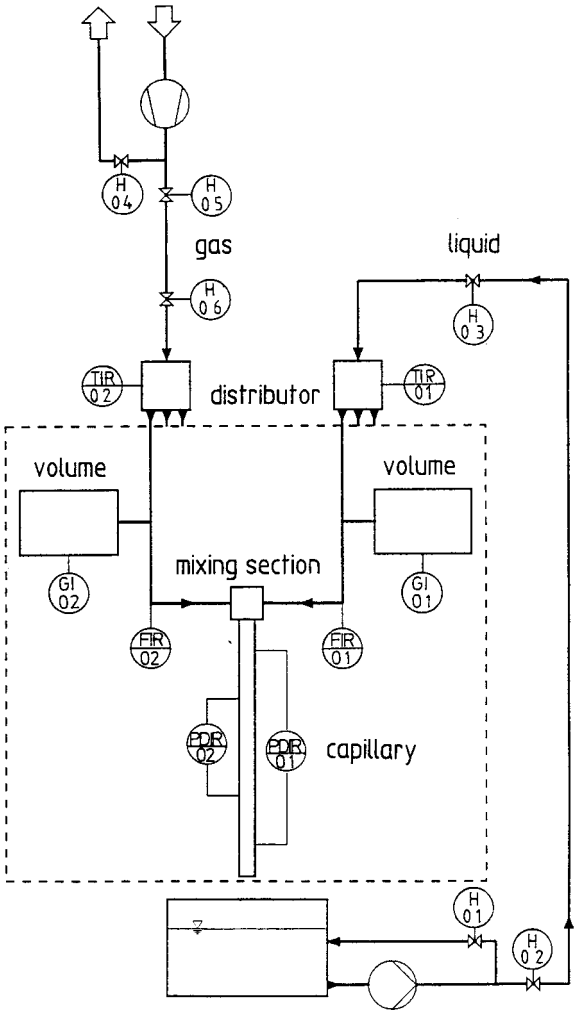

Fig. 3. Schematical representation of the experimental set-up.

equipped with pressure taps for differential pressure measurements along two different lengths as well as conductive sensors for the void fraction. In Fig. 4 the pressure tap (Fig. 4a) and the void fraction sensor (Fig. 4b) are schematically depicted. The liquid and the gaseous phase are fed into a mixing section located at the top of the capillary tube. A storage container at the end of the tube is used for the separation of the two phases. While the liquid is recirculated using a pump, the gaseous phase is supplied by a compressor and discharged.

The feed systems for the gas and liquid phases are equipped with a fixed and very high stationary pressure drop from valves which are used to decouple the oscillations of the system pressure drop in the test section from the feed characteristics of the pump and the compressor. In the feed lines to the mixing section a buffer volume of variable size is included. Whereas the

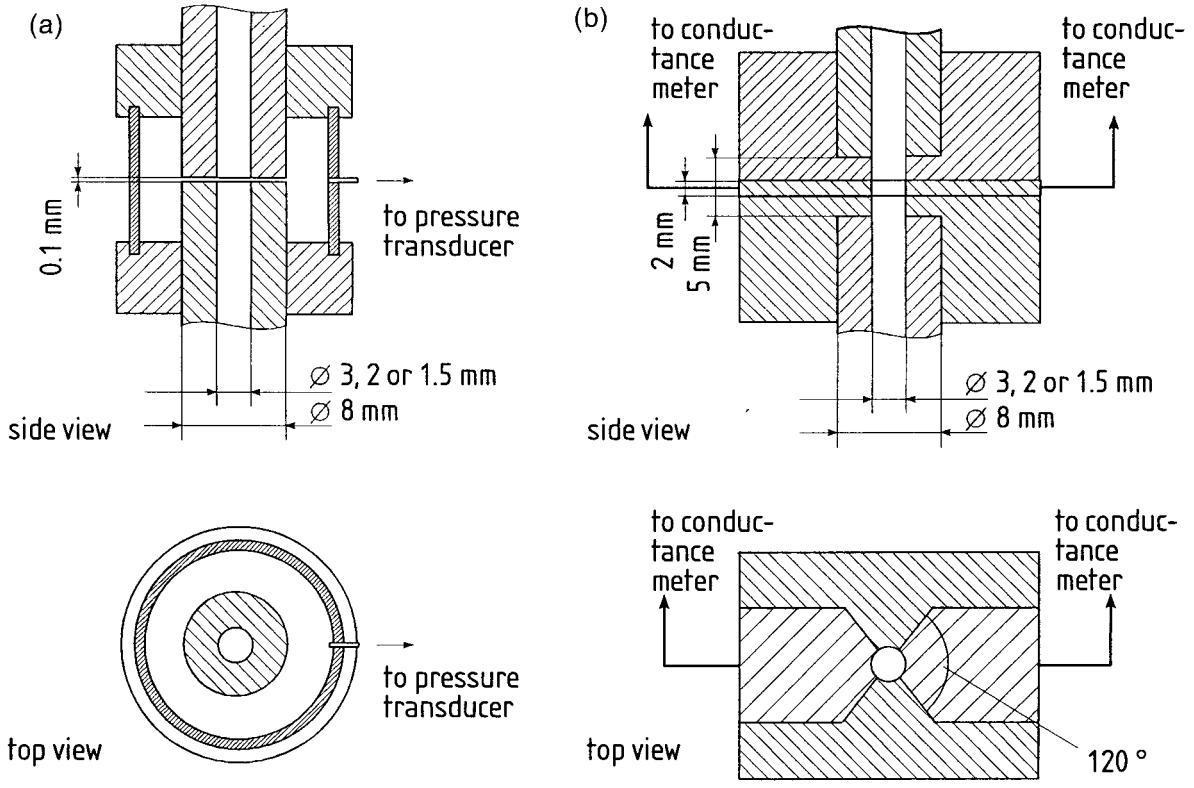

Fig. 4. Schematical repesentation of (a) the pressure taps and (b) the void fraction sensors.

gaseous phase is already compressible, the buffer volume in the liquid section of the feed line contains a gas bubble of variable size yielding the compressible properties.

4.1. Stationary experiments

For pressure drop oscillations to be possible, instabilities in the stationary pressure drop characteristic have to be identified. This can be achieved, as has been shown in the previous section, when no compressibilities are present in the feed pipes. Therefore, in a first set of experimental investigations the compressible volumes in both feed lines were removed in order to facilitate the measurement of the stationary pressure drop across the test section as a function of the volumetric flow rate of the gaseous and the liquid phase.

In Fig. 5, the pressure drop per unit length across the capillary is plotted as a function of the volumetric gas flow rate for three volumetric liquid flow rates. The capillary used has an inner diameter of 3 mm. The plotted pressure drop is measured from the mixing section down in the direction of the flow. Therefore, for small gas flow rates up to superficial velocities of $j_G = 0.35$ m/s (corresponding to Reynolds numbers of the gaseous phase Re_G of 70), the pressure drop is negative. This holds true for all the liquid flow rates depicted. This is due to the fact that the overall pressure drop is dominated by the hydrostatic pressure drop, which in turn is negative.

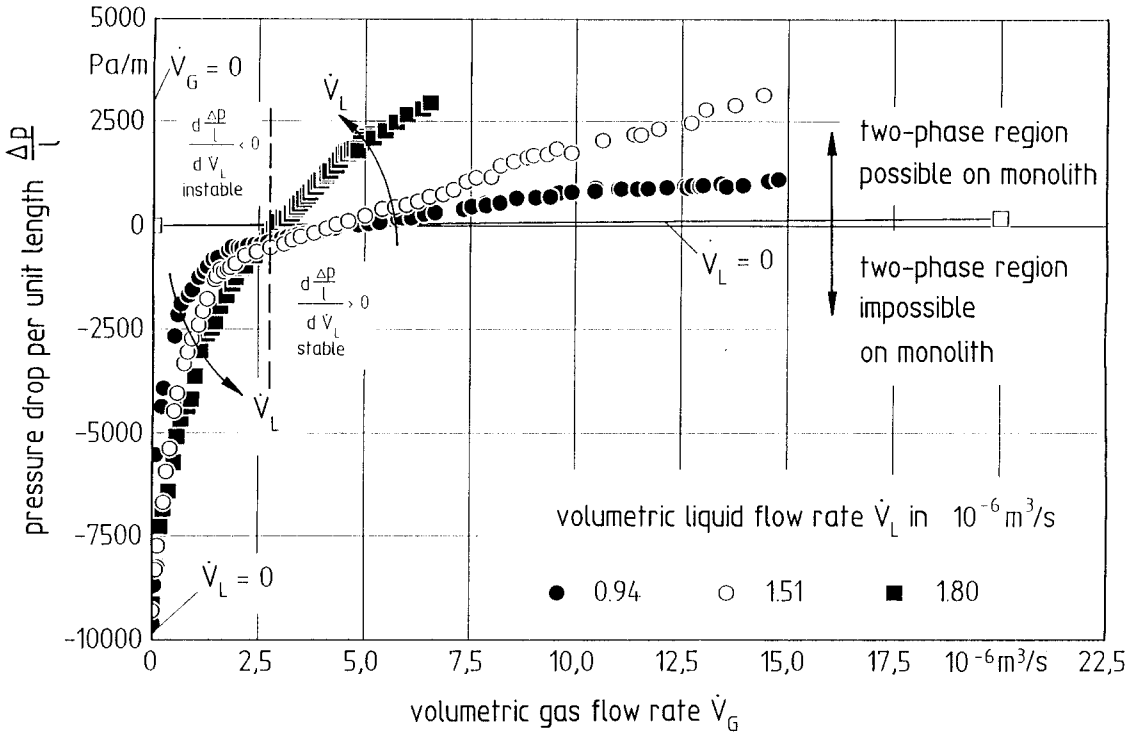

Fig. 5. The pressure drop per unit length as a function of the volumetric gas flow rate for three different volumetric liquid flow rates (single capillary, $d = 3$ mm).

For higher gas flow rates, the system is dominated by the frictional pressure drop and the overall pressure drop thus is positive. In the region, where the pressure drop is dominated by the hydrostatic pressure drop, an increase of the volumetric liquid flow rate for constant gas flow rates will yield a decrease of the void fraction in the capillary. The increase of the liquid flow rate ranges from superficial velocities of $j_L = 0.1$, 0.2 and 0.25 m/s (corresponding to Reynolds numbers of the liquid phase Re_L of 380, 630, and 750, respectively). Thus, the hydrostatic pressure drop is increased and the overall pressure drop decreased. Therefore, in this region

$$\mathrm{d}\frac{\frac{\Delta p}{l}}{\mathrm{d}\dot{V}_L} < 0 \tag{18}$$

and the system displays instabilities in reference to the liquid phase. Within Eq. (18), $\dot{V}_L$ is the volumetric flow rate of the liquid phase. These instabilities will, when the system is coupled with compressibilities, generate pressure drop oscillations.

In Fig. 6, the pressure drop per unit length across the capillary is plotted as a function of the volumetric gas flow rate for one volumetric liquid flow rate. The parameter in this plot is the degree of turbulence of the liquid phase at the inlet of the test section. The turbulence was generated by bubbles of different sizes in the mixing inlet of the liquid phase. For a high

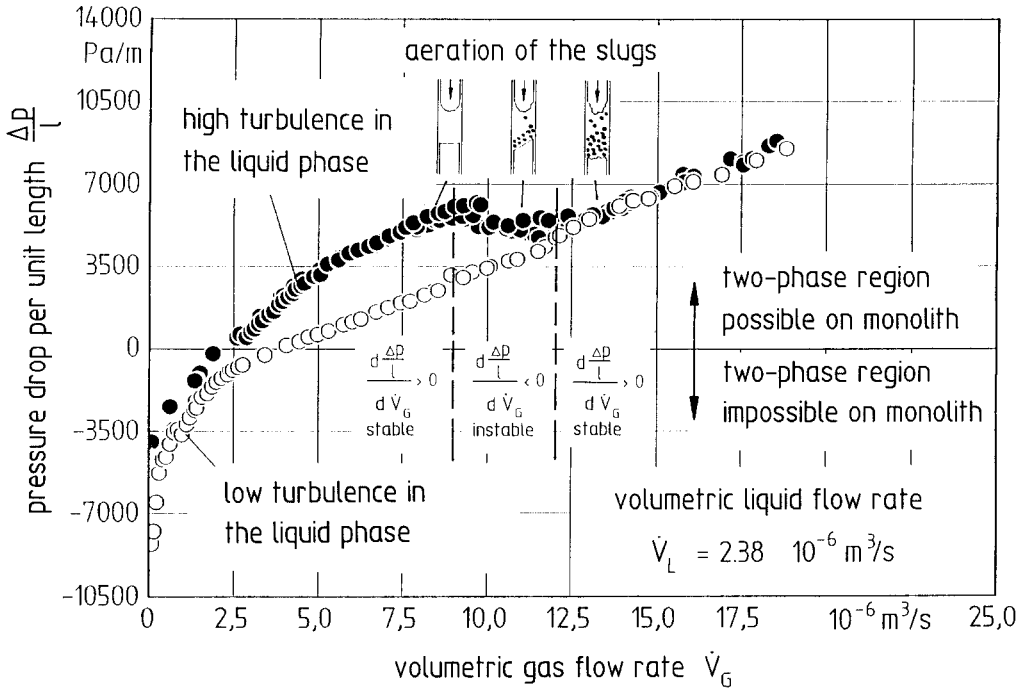

Fig. 6. The pressure drop per unit length as a function of the volumetric gas flow rate for one volumetric liquid flow rate (single capillary, $d = 3$ mm).

degree of turbulence in the liquid phase and small or intermittent gas flow rates, the pressure drop per unit length is significantly higher than for the flow with the smaller degree of turbulence in the liquid phase. This effect is due to an increase of the slug frequency due to the turbulence in the liquid phase. With the same liquid flow rate, an increase in the slug frequency will result in a decrease of the slug length. Since the slugs and in particular the front of the slugs, where due to the turbulence in the liquid phase the velocity gradients are large, are responsible for the frictional pressure drop, an increase of the number of slugs will automatically lead to an increase of the frictional pressure drop.

For a superficial velocity of the gas of approximately $j_G = 1.4$ m/s (corresponding to Reynolds numbers of the gaseous phase Re_G of 270) and a high degree of turbulence in the liquid phase the pressure drop decreases. This is due to the transition from the slug flow regime to the aerated slug flow regime, which is shown in Fig. 7 for increasing gas flow rates. Similar effects have been reported by other authors for the horizontal two-phase flow including Andreussi and Bendiksen (1989), Nydal and Andreussi (1991), Barnea and Brauner (1985) and Obot et al. (1991). As small gas bubbles are entrained into the front of the slug, the homogeneous viscosity decreases. Since the viscosity is directly proportional to the shear stress and thus the pressure drop, the frictional pressure drop will also decrease. This decrease in the pressure drop can be written as

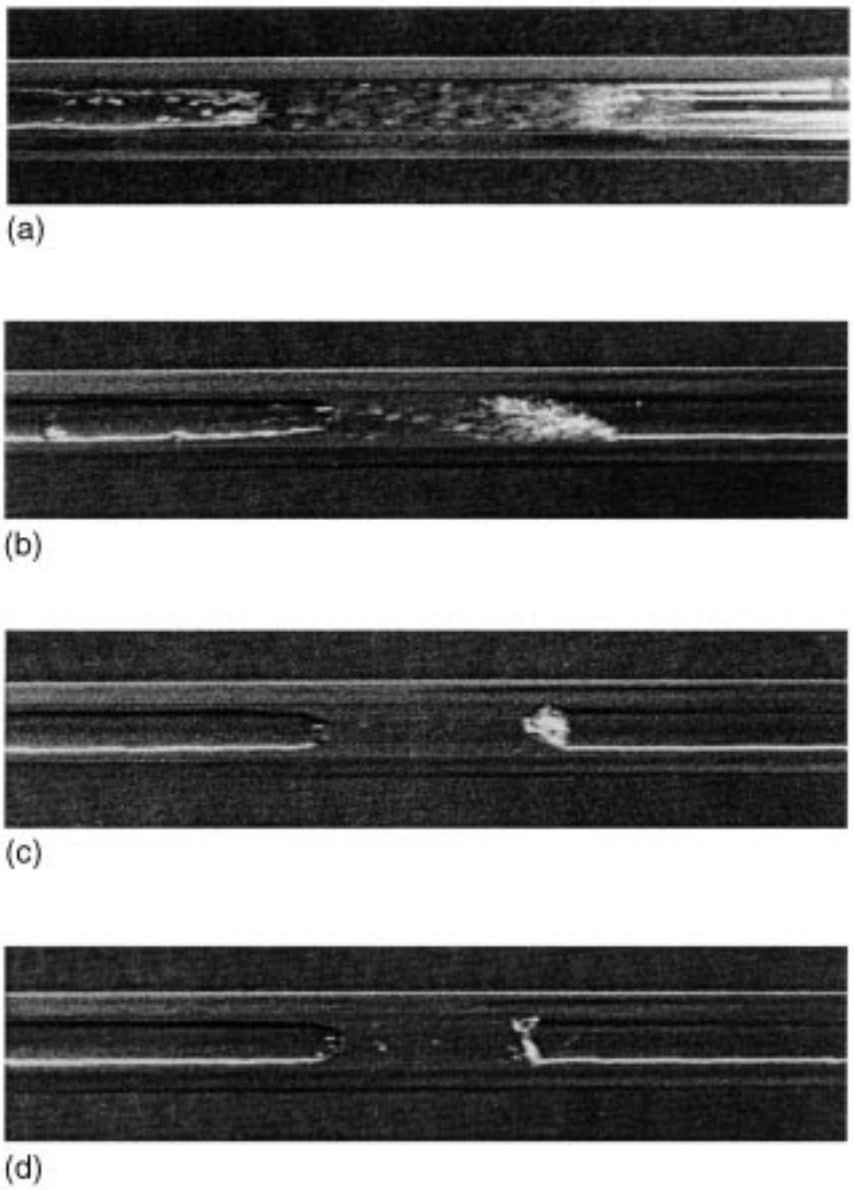

Fig. 7. Photos of liquid slugs flowing from top to bottom. The gas flow rate is increased from (a) to (d) and aeration of the slugs occurs.

$$\mathrm{d}\frac{\frac{\Delta p}{l}}{\mathrm{d}\dot{V}_{\mathrm{G}}}<0 \tag{19}$$

$\dot{V}_{\mathrm{G}}$ is the volumetric flow rate of the gaseous phase. For the condition given in [19], the system

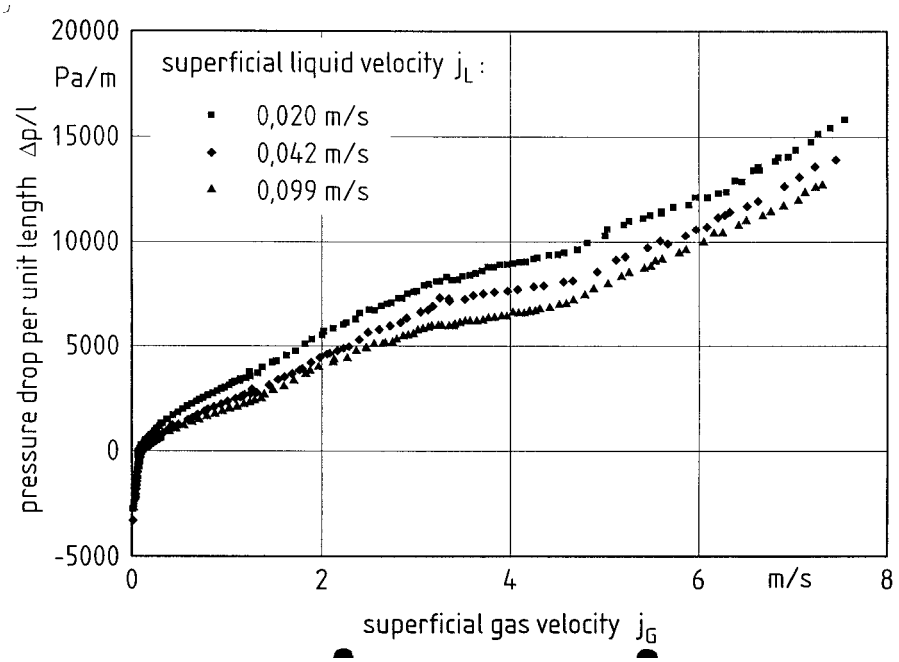

Fig. 8. The pressure drop per unit length as a function of the volumetric gas flow rate for three different volumetric liquid flow rates (monolith, $d = 1.19$ mm).

displays pressure drop instabilities. When the maximum aeration of the slug is reached, the local minimum is passed and the system is again stable.

In order to assess, whether a similar behaviour of the two-phase flow in monolithic catalyst supports is observed as has been shown for the single capillary, measurements were conducted using an array of ceramic monolithic catalyst supports with 118 mm outer diameter, 300 cpi (cells per in.^{2}) and 10.5 ml (10^{-3} in.) wall thickness. The shape of the channels is square resulting in a hydraulic diameter of 1.19 mm. The measurements were conducted using a total length of the test section of 960 mm. In Fig. 8, results for the pressure drop per unit length as a function of the gas flow rate for several liquid flow rates are plotted. It is evident, that both instabilities found in the single channel experiments are also present in the cocurrent two-phase flow of the monolithic catalyst supports. Therefore, the transient behaviour of the flow through the multichannel catalyst is expected to be similar to the transient behaviour of the flow through the capillary.

4.2. Transient experiments

When adding compressible volumes to the feed lines of the two phases, pressure drop oscillations can be observed. A requirement for the development of pressure drop oscillations is the operation of the test section in the instable regions of the pressure drop curve.

In Fig. 9, sample oscillations for instabilities in reference to the gaseous phase are shown. Plotted are in Fig. 9a the volumetric gas flow rate, in Fig. 9b the volumetric liquid flow rate

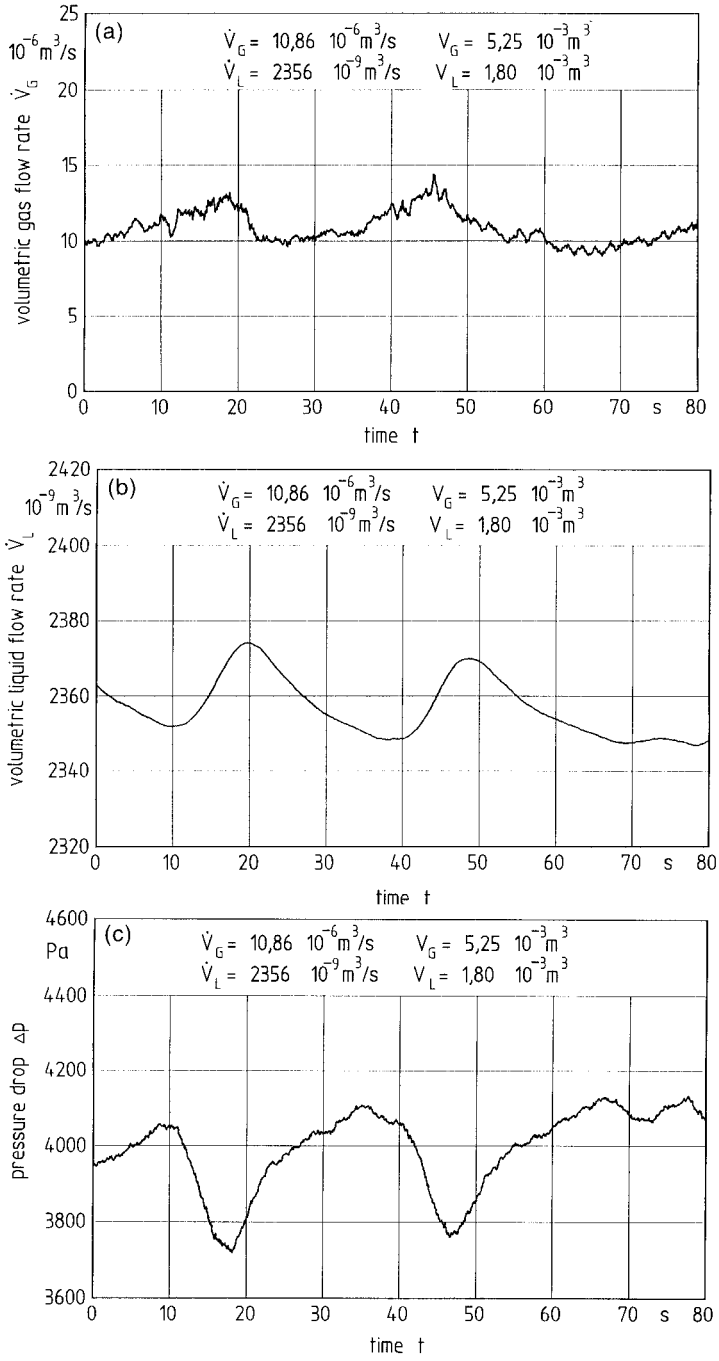

Fig. 9. Sample results of oscillations resulting from instabilities in reference to the gaseous phase: (a) volumetric gas flow rate, (b) volumetric liquid flow rate and (c) pressure drop all as a function of time (single capillary, $d = 3$ mm).

and in Fig. 9c the pressure drop as a function of time. The parameters for the average flow rates of both phases and the size of the buffer volumes are given in the legend. The corresponding superficial velocities are $j_G = 1.45$ m/s ($Re_G = 300$) for the gaseous phase and $j_L = 0.34$ m/s ($Re_L = 1000$) for the liquid phase. It was found experimentally, that for an increase in compressible volume of either phase, the frequency of the oscillations decreases. This is in accordance with the simple theory given above. The phase difference between the oscillations of the liquid phase and the gaseous phase is increased with increasing liquid buffer volume. This is due to the higher storage capabilities in the liquid feed line and the longer times for the change of flow direction into or from the buffer volume.

In Fig. 10, sample oscillations for instabilities in reference to the liquid phase are shown. Plotted are in Fig. 10a the volumetric gas flow rate, in Fig. 10b the volumetric liquid flow rate, and in Fig. 10c, the pressure drop as a function of time. The parameters for the average flow rates of both phases and the size of the buffer volumes are given in the legend. The corresponding superficial velocities are $j_G = 0.3$ m/s ($Re_G = 57$) or the gaseous phase and $j_L = 0.23$ m/s ($Re_L = 657$) for the liquid phase. It was found experimentally, that for an increase of the size of the buffer volumes of the gaseous phase the frequency of the oscillations is decreased, whereas for an increase of the size of the buffer volumes of the liquid phase, the frequency of the oscillations is increased. While the first finding is in accordance with the simple theory given above. The second finding shows that there are oversimplifications in the model. Therefore, a more detailed model has to be developed.

5. Theoretical investigations

In the theoretical investigations on the pressure drop oscillations of the cocurrent vertical downflow of a gaseous and a liquid phase presented in this paper, we will focus on the instabilities in reference to the gaseous phase.

In order to mathematically describe the complete system by a set of differential equations with the corresponding boundary conditions, each component of the feed lines and the test section has to be taken and modelled. The simplest way to do this, as has been described in Section 3, is to use integral equations. Thus the pipes were modelled with a simple laminar/turbulent pressure drop law, where a continuous transition was included to avoid mathematical instabilities. The equation then becomes

$$\Delta p = \frac{\rho}{2d}\left(\frac{\dot{V}}{A}\right)^2 \psi + \frac{\rho}{A}\frac{\mathrm{d}\dot{V}}{\mathrm{d}t} \quad \textit{and} \quad \psi = \sqrt{\left(\frac{64}{Re}\right)^2 + \left(\frac{0.3164}{Re^{0.25}}\right)^2} \tag{20}$$

which is in accordance to the general form given in Eq. (2). The compressibilities of the buffer volumes were modelled using the ideal gas law, as has been given in Eq. (7). This is valid for the gaseous phase. Since the liquid phase is incompressible in the pressure ranges investigated, a gas bubble is used to yield the compressible effect in the feed pipes. Therefore, Eq. (2) has to be modified. It then becomes

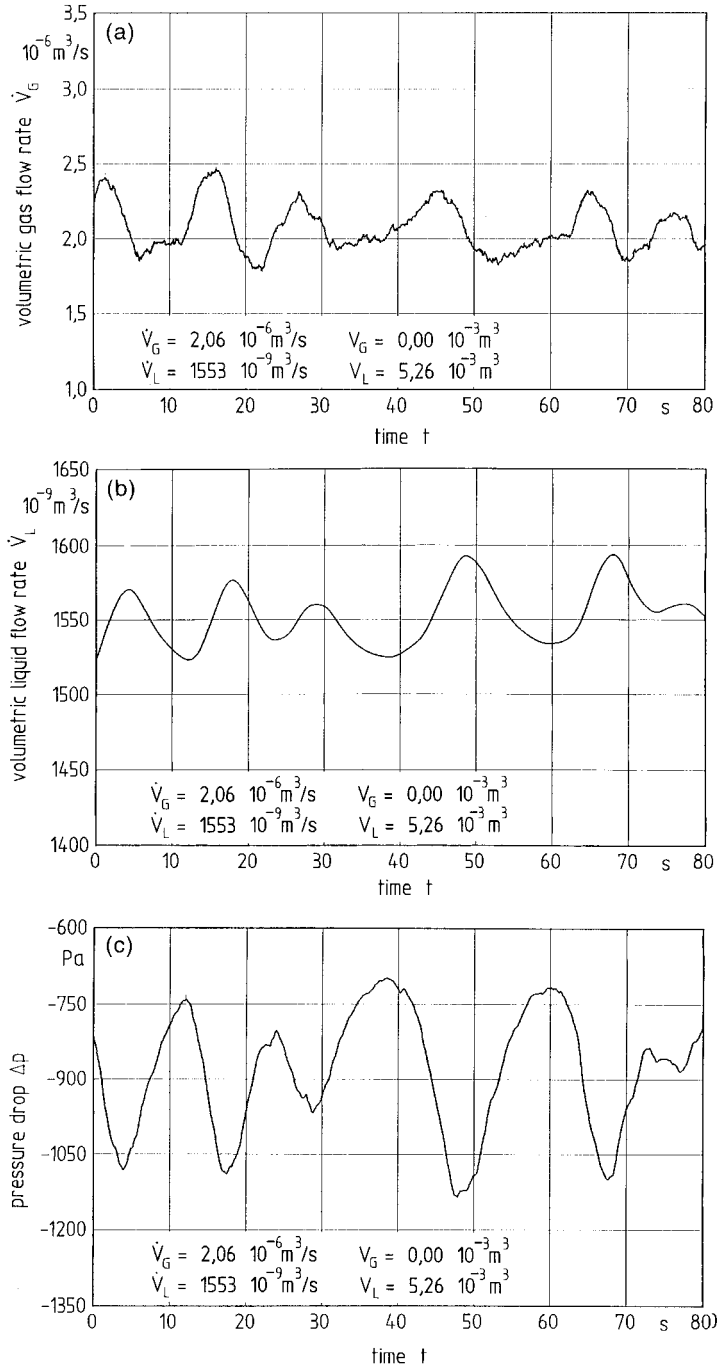

Fig. 10. Sample results of oscillations resulting from instabilities in reference to the liquid phase: (a) volumetric gas flow rate, (b) volumetric liquid flow rate and (c) pressure drop all as a function of time (single capillary, $d = 3$ mm).

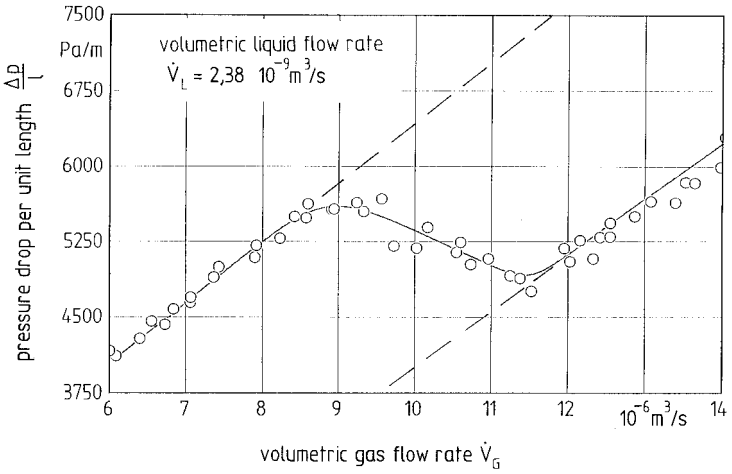

Fig. 11. The pressure drop per unit length as a function of the volumetric gas flow rate for one volumetric liquid flow rate in the instable region of the gas flow rate (single capillary, $d = 3$ mm).

$$\frac{\mathrm{d}}{\mathrm{d}t}\left(\frac{1}{p}\right) = -\dot{V}_{\mathrm{L}}\frac{1}{p_0 V} \tag{21}$$

Due to inverse of the pressure on the LHS of Eq. (21), the stepwidth of the calculation has to be chosen so that no mathematical instability arises, yet the time resolution is high enough for the transient oscillations.

Closing equations were obtained at the junctions and the feed flow rates from the pump and the compressor were assumed to be constant.

The pressure drop instability in the aerated slug flow regime was modelled using the correlation by Storek and Brauer (1980) and including an additional curve fit for the data:

$$\Delta p = \Delta p_{\mathrm{STAT}} + \frac{1}{A}\left[\rho_{\mathrm{L}}\frac{\mathrm{d}\dot{V}_{\mathrm{L}}}{\mathrm{d}t} + \rho_{\mathrm{G}}\frac{\mathrm{d}\dot{V}_{\mathrm{G}}}{\mathrm{d}t}\right] \quad \textit{and} \quad \Delta p_{\mathrm{STAT}} = f\left(\dot{V}_{\mathrm{L}}, \dot{V}_{\mathrm{G}}\right) \tag{22}$$

The correlation and the experimental data for one exemplary operating point are shown in Fig. 11, where the stationary pressure drop per unit length Δp_{STAT} is plotted as a function of the volumetric gas flow rate $\dot{V}_{\mathrm{G}}$ for one volumetric liquid flow rate $\dot{V}_{\mathrm{L}}$. The inertia of the two-phase system was included in accordance to the inertia of the feed pipes.

The resulting differential equation is strongly non-linear and of second order. Solving the equation with standard methods was found to be unsuccessful. Therefore, a dynamic finite step numerical scheme was developed to solve the equation.

In Fig. 12 sample experimental results for the pressure drop oscillations are compared to the numerical results obtained from the model described. Plotted is the pressure drop as a function of time for the operating parameters given in the legend. The corresponding superficial velocities are $j_{\mathrm{G}} = 1.8$ m/s ($Re_{\mathrm{G}} = 353$) for the gaseous phase and $j_{\mathrm{L}} = 0.34$ m/s ($Re_{\mathrm{L}} = 1000$) for the liquid phase. The agreement between the numerical and the experimental results is good, not only for the frequency and the amplitude of the oscillations, but also for the shape of the pressure drop trace.

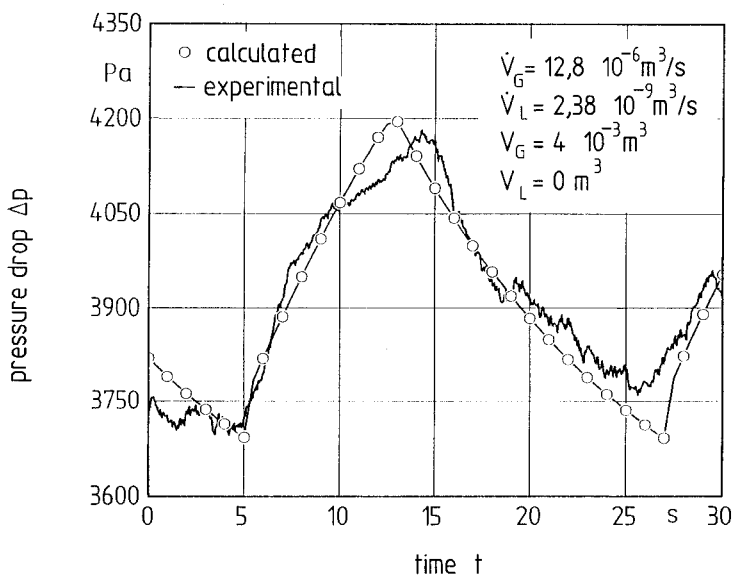

Fig. 12. The pressure drop for an oscillation due to an instability in reference to the gaseous phase as a function of time (single capillary, $d = 3$ mm).

In Fig. 13 the calculated frequency of the oscillations is plotted as a function of the volumetric gas flow rate for one volumetric liquid flow rate. The corresponding superficial velocity is $j_L = 0.34$ m/s ($Re_L = 1000$). The parameter in this plot is the size of the buffer

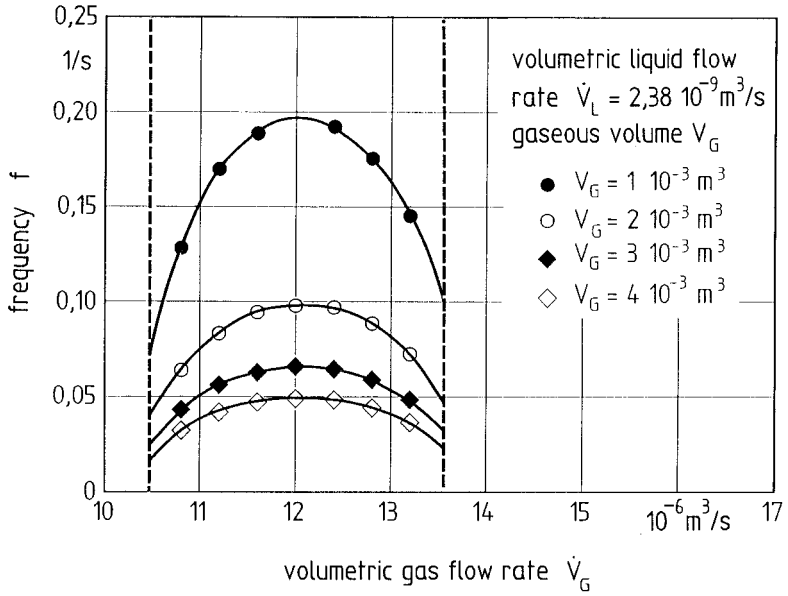

Fig. 13. The frequency of the oscillations as a function of the volumetric gas flow rate for the operating condition given in the legend (single capillary, $d = 3$ mm).

volume in the gaseous feed line. The buffer volume in the liquid feed line is zero. The vertical lines indicate the limit of the region of instability. The frequency of the oscillations is increased for decreasing sizes of the buffer volume in the gaseous feed line. This is in accordance with the simple model developed in Section 3. As was expected from the results plotted in Fig. 12 the agreement between measured and calculated results is good. The onset of the oscillations, when changing the gas flow rate from a stable operating point to an instable operating point is spontaneous. The frequency of the pressure drop oscillations is increased in the middle of the instable region. Here, the negative slope of the pressure drop becomes larger and therefore the acceleration of the fluids greater. With greater acceleration, the frequency of the oscillations also becomes larger. This finding is in accordance to the simple model developed in Section (3).

6. Conclusions

Transient flows in single capillaries with a two-phase cocurrent downflow of a gaseous and a liquid phase were studied. The goal of the investigation was the estimation of transient flow oscillations in monolithic catalyst supports. As a model for a single channel, a capillary tube was used. The experimental investigations showed instabilities both regarding the liquid and the gaseous phase. A mathematical model was developed for the calculation of the pressure drop oscillations. The differential equation that was derived is a second-order, non-linear equation. Solving of the equation was done by using a dynamic finite step numerical scheme. The agreement of the numerical results and the experimental data for the oscillations is good, not only for the frequency and amplitude of the oscillations, but also for the shape of the oscillations. Further work needs to be done to verify the model with oscillations obtained for the two-phase flow in monolithic catalyst supports, where the same instabilities are found.

Acknowledgements

The authors wish to thank the German Research Foundation (Deutsche Forschungsgemeinschaft, DFG) for the financial support of the investigations.

References

Andreussi, P., Bendiksen, K., 1989. An investigation of void fraction in liquid slugs for horizontal and inclined gas–liquid pipe flow. Int. J. Multiphase Flow 15 (6), 937–946.

Barnea, D., Brauner, N., 1985. Holdup for the liquid slug in two-phase intermittend flow. Int. J. Multiphase Flow 11 (1), 43–49.

Beretta, A., Tronconi, E., Alemany, L.J., Svachula, J., Forzatti, P., 1993. Effect of morphology on the reduction of NO_x and the oxidation of SO_2 over honeycomb SCR catalysts. In: Proceedings II World Congress and VI European Workshop Meeting, New Developments in Selective Oxidation. Elsevier.

Chou, T.S., Worley, F.L., Luss, D., 1977. Transition to pulsed flow in mixed-phase cocurrent downflow through a fixed bed. Ind. Eng. Chem. Proc. Des. Dev. 16 (3), 424–427.

Crynes, L.L., Cerro, R.L., Abraham, M.A., 1995. Monolith froth reactor: development of a novel three-phase catalytic system. AIChE J. 42 (2), 337–345.

Gianetto, A., Baldi, G., Specchia, V., Sicardi, S., 1978. Hydrodynamics and solid–liquid contacting effectiveness in trickle-bed reactors. AIChE J. 24 (6), 1087–1104.

Gianetto, A., Specchia, V., 1992. Trickle-bed reactor: state of the art and perspectives. Chem. Eng. Sci. 47 (13/14), 3197–3213.

Grosser, K., Carbonell, R.G., Sundaresan, S., 1988. Onset of pulsing in two-phase cocurrent downflow through a packed bed. AIChE J. 34 (11), 1850–1860.

Hatziantoniou, V., Anderson, B., 1982. Solid–liquid mass transfer in segmented gas–liquid flow through a capillary. Ind. Eng. Chem. Fundam. 21, 451–456.

Hatziantoniou, V., Anderson, B., 1984. The segmented two-phase flow monolithic reactor. An alternative for liquid-phase hydrogenations. Ind. Eng. Chem. Fundam. 23, 82–88.

Holub, R.A., Dudukovic, M.P., Ramachandran, P.A., 1992. A phenomenological model for pressure drop, liquid holdup and flow regime transition in gas–liquid trickle flow. Chem. Eng. Sci. 47 (9/11), 2343–2348.

Holub, R.A., Dudukovic, M.P., Ramachandran, P.A., 1993. Pressure drop, liquid holdup and flow regime transition in trickle flow. AIChE J. 39 (2), 302–321.

Irandoust, S., Anderson, B., 1988. Mass transfer and liquid-phase reactions in a segmented two-phase flow monolithic catalyst reactor. Chem. Eng. Sci. 43 (8), 1983–1988.

Irandoust, S., Anderson, B., 1989a. Simulation of flow and mass transfer in Taylor flow through a capillary. Comp. Chem. Engng. 13 (4/5), 519–526.

Irandoust, S., Anderson, B., 1989b. Liquid film in Taylor flow through a capillary. Ind. Eng. Chem. Res. 28, 1684–1688.

Irandoust, S., Andersson, B., Bengtsson, E., Siverström, M., 1989. Scaling up of a monolithic catalyst reactor with two-Phase flow. Ind. Eng. Chem. Res. 28, 1489–1493.

Irandoust, S., Gahne, O., 1990. Competitive hydrodesulfurization and hydrogenation in a monolithic reactor. AIChE J. 36 (5), 746–752.

Kariyasaki, A., Fukano, T., Kagawa, M., Ousaka, A., 1991. Void fraction, bubble length and liquid film thickness in isothermal air–water cocurrent flow in a horizontal capillary tube. In: Proceeding of the Int Conference on Multiphase Flow '91, Tsukuba, 24–27 Sept, 471–474.

Kawakami, K., Kawasaki, K., Shiraishi, F., Kusunoki, K., 1989. Performance of a honeycomb monolith bioreactor in a gas–liquid–solid three-phase system. Ind. Eng. Chem. Res. 28, 394–400.

Marchessault, R.N., Mason, S.G., 1960. Flow of entrapped bubbles through a capillary. Ind. Eng. Chem. 52 (1), 79–84.

Morsi, B.I., Laurent, A., Midoux, N., Barthole-Delauney, G., Storck, A., Charpentier, J.-C., 1984. Hydrodynamics and gas–liquid–solid interfacial parameters of cocurrent downward two-phase flow in trickle-bed reactors. Chem. Eng. Commun. 25, 267–293.

Nydal, O.J., Andreussi, P., 1991. Gas entrainment in a long liquid slug advancing in a near horizontal pipe. Int. J. Multiphase Flow 17 (2), 179–189.

Obot, N.T., Wambsganss, M.W., France, D.M., 1991. A generalized method for correlation of adiabatic two-phase flow frictional pressure drop data. AIChE Symp. Ser 87 (283), 289–298.

Ozawa, M., Akagawa, K., Sakaguchi, T., Tsukahara, T., Fujii, T., 1979a. Oscillatory flow instabilities in air–water two-phase flow systems. Bull. JSME 22 (174), 1763–1770.

Ozawa, M., Nakanishi, S., Ishigai, S., 1979b. Flow instabilities in multi-channel boiling systems. Trans. ASME 79-WA/HT 55, 1–7.

Ozawa, M., Nakanishi, S., Ishigai, S., Mizuta, Y., Taruili, H., 1979c. Flow instabilities in boiling channels; Part I: Pressure drop oscillations. Bull. JSME 22 (17), 1113–1118.

Ozawa, M., Akagawa, K., Sakaguchi, T., Tsukahara, T., Suezawa, T., 1982. Oscillatory flow instabilities in a gas–liquid two-phase flow system. In: Bankhoff, S.G., Afgan, N.H. (Eds.), Heat Transfer in Nuclear Reactor Safety. Hemisphere, Washington, DC, pp. 379–390.

Ozawa, M., Akagawa, K., Sakaguchi, T., 1984. Flow instabilities in parallel-channel flow systems of gas–liquid two-phase mixtures. Int. J. Multiphase Flow 15 (4), 639–657.

Sai, P.S.T., Varma, Y.B.G., 1988. Flow pattern of the phases and liquid saturation in gas–liquid cocurrent downflow through packed beds. Can. J. Chem. Eng. 66, 353–360.

Satterfield, C.N., Özel, F., 1977. Some characteristics of two-phase flow in monolithic catalyst structures. Ind. Eng. Chem. Fundam. 16 (1), 61–67.

Storek, H., Brauer, H., 1980. Reibungsdruckverlust der adiabaten Gas/Flüssigkeitsströmung in horizontalen und vertikalen Rohren. VDI-Forschungsheft 599.

Suo, M., 1968. Pressure drop in capillary slug flow. Trans. ASME 3, 140–141.

Suo, M., Griffth, P., 1964. Two-phase flow in capillary tubes. Trans. ASME 9, 576–582.

Svachula, J., Alemany, L.J., Ferlazzo, N., Forzatti, P., Tronconi, E., Bergani, F., 1993a. Oxidation of S to SO_3 over honeycomb denoxing catalysts. Ind. Eng. Chem. Res. 32, 826–834.

Svachula, J., Ferlazzo, N., Forzatti, P., Tronconi, E., Bergani, F., 1993b. Selective reduction of NO_x by NH_3 over honeycomb SCR catalysts. Ind. Eng. Chem. Res. 32, 1053–1060.

Talmor, E., 1977. Two-phase downflow through catalyst beds. AIChE J. 23 (6), 868–878.

Thulasidas, T.C., Abraham, M.A., Cerro, R.L., 1995. Bubble-train flow in capillaries of circular and square cross section. Chem. Eng. Sci. 50 (2), 183–199.

Tronconi, E., Beretta, A., Forzatti, P., Malloggi, S., Dé Michele, G., 1991. A mathematical model of the monolith reactor for selective catalytic removal of NO_x. Atti Convegno Nazinale Tecnologie Chimiche nella Produzione di Energia Elettrica. Pisa, 29–30 Oct., pp. 417–427.

Tronconi, E., Forzatti, P., 1992. Adequacy of lumped parameter models for SCR reactors with monolith structure. AIChE J. 38, 201–210.